Supporting Information

Ultralight, Highly Compressible, Thermally Stable MXene/Aramid Nanofibers Anisotropic Aerogels for Electromagnetic Interference Shielding

Yiqian Du, Jian Xu, Jiangyu Fang, Yantai Zhang, Xiaoyun Liu[*]*, Peiyuan Zuo, Qixin Zhuang*[*]

[a]Key Laboratory of Specially Functional Polymeric Materials and Related Technology (Ministry of Education), School of Material Science and Engineering, East China University of Science and Technology, Shanghai 200237, P. R. China

[*]Email: qxzhuang@ecust.edu.cn

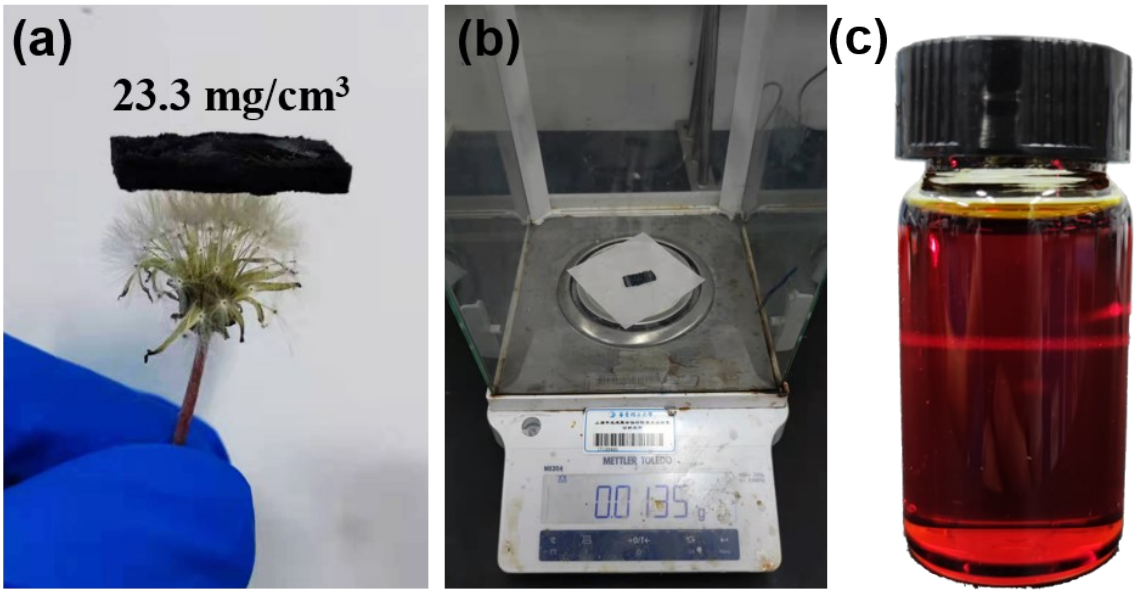

Figure S1. (a) Digital photo of ATA-5 on a dandelion and (b) Ultralight ATA-5 on precision balances. (c) Digital photograph of ANFs colloid showing the Tyndall effect.

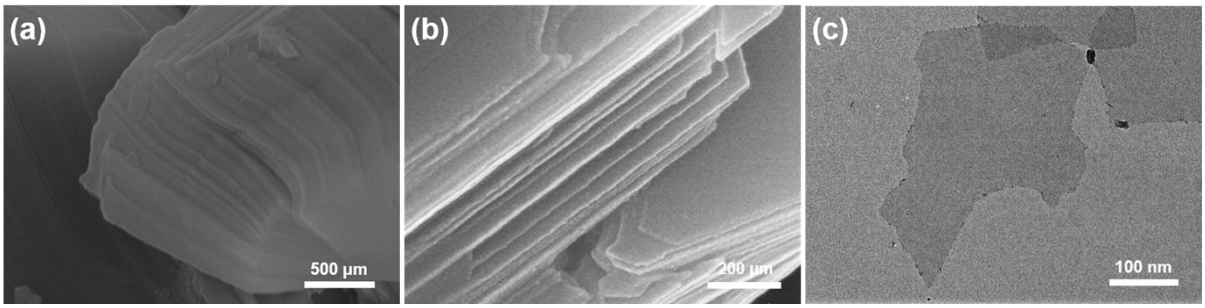

Figure S2. (a) SEM image of Ti_3AlC_2 and (b) SEM image of Clay-like $Ti_3C_2T_x$ MXene particle obtained after etching and (c) TEM image of $Ti_3C_2T_x$ nano sheets.

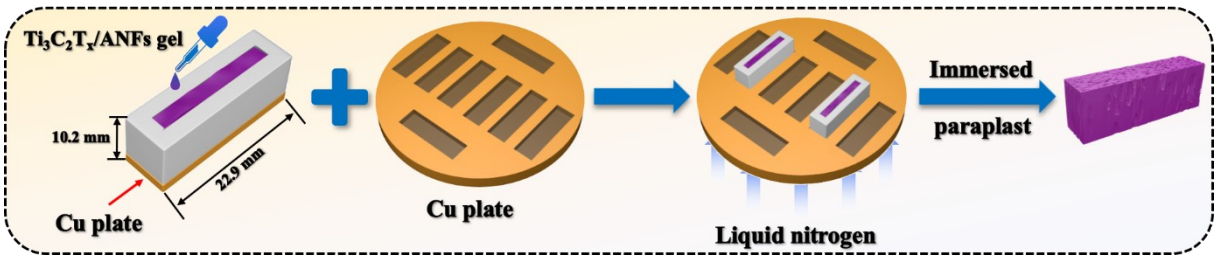

Figure S3. Schematic diagram of sample preparation of anisotropic $Ti_3C_2T_x$/ANF aerogel for electromagnetic shielding test.

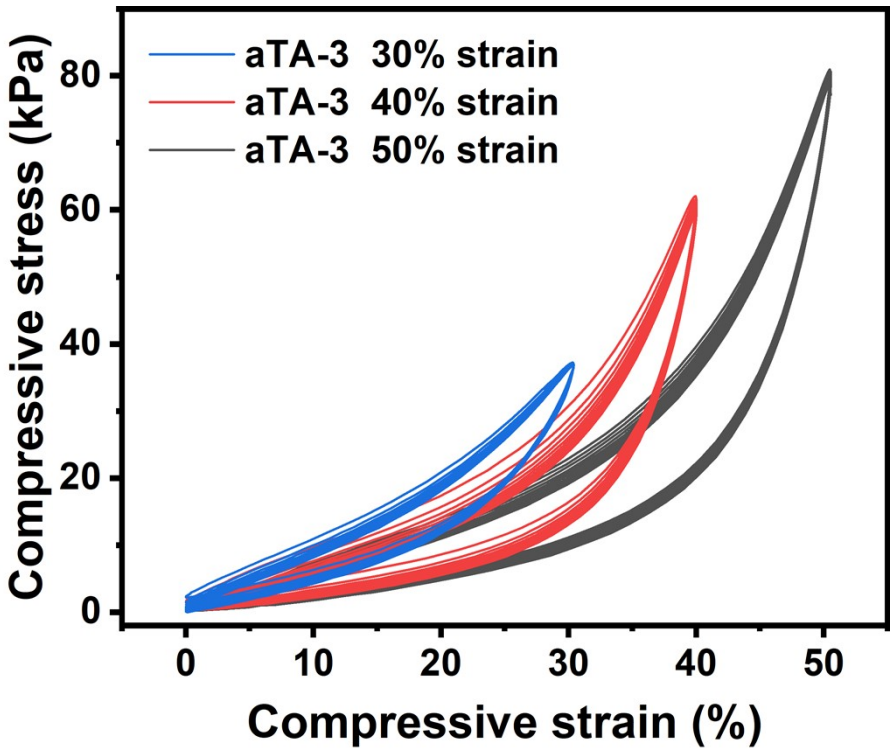

Figure S4. Stress-strain curves for 10 compression cycles of aTA-3 at 30%, 40% and 50% compressive strain.

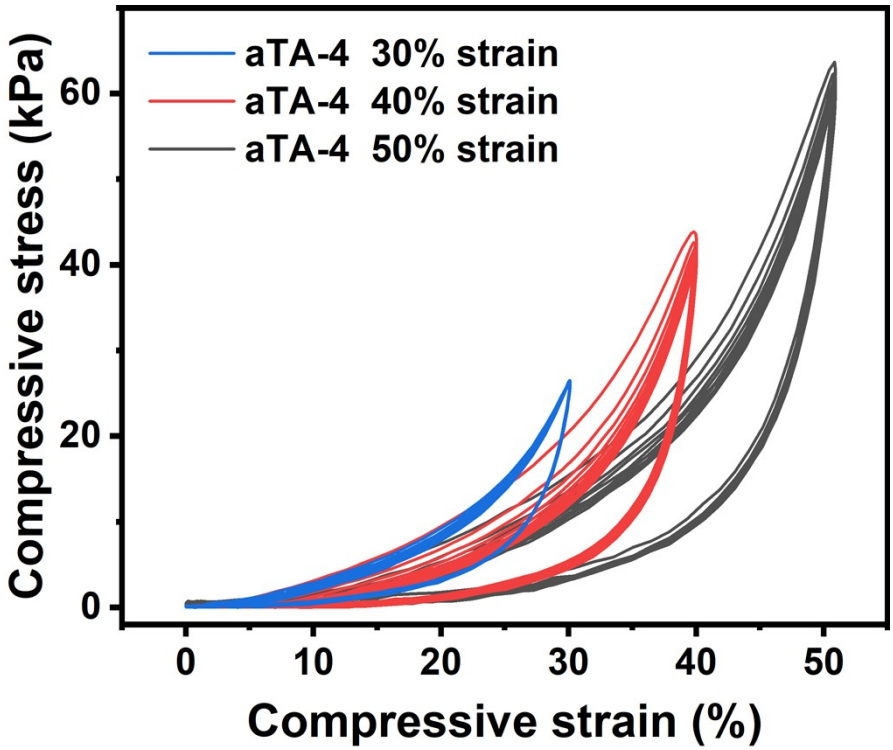

Figure S5. Stress-strain curves for 10 compression cycles of aTA-4 at 30%, 40% and 50% compressive strain.

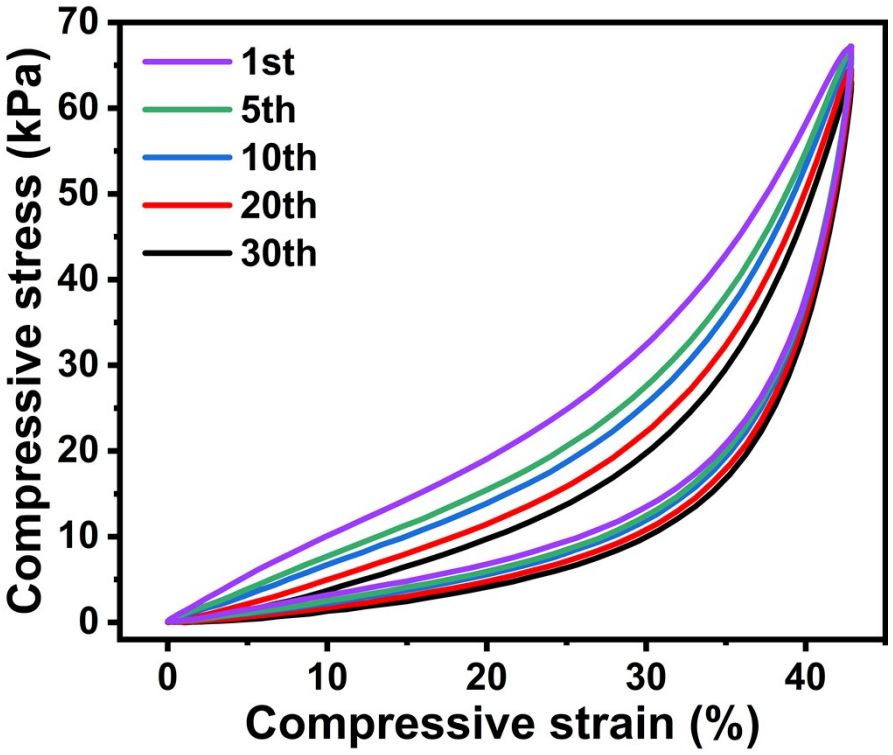

Figure S6. Stress-strain curves of aTA-2 with 30 compression cycles along the vertical direction.

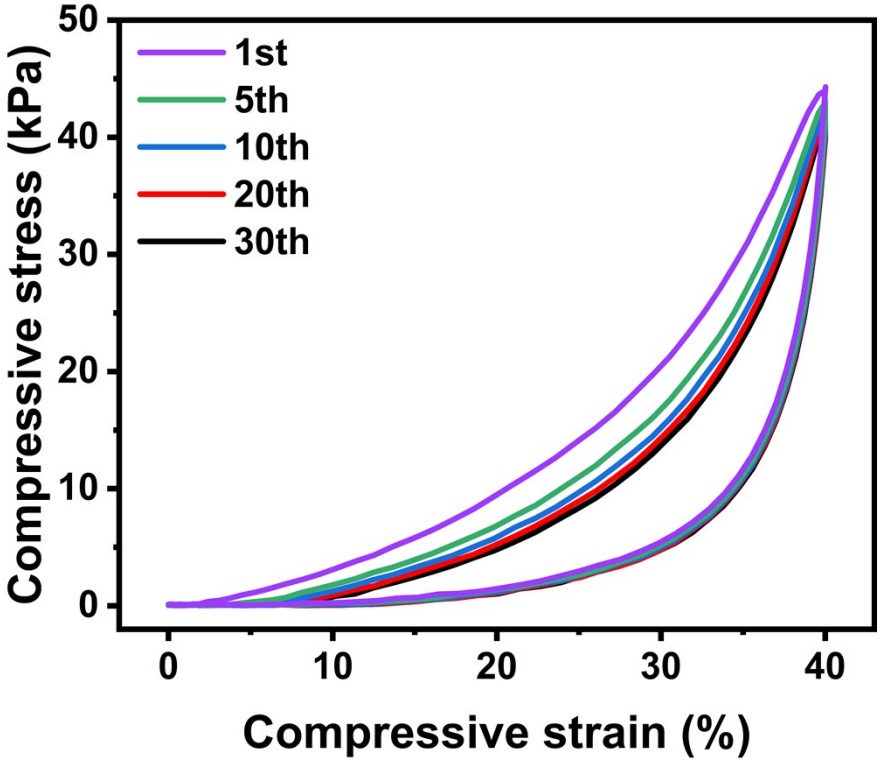

Figure S7. Stress-strain curves of aTA-4 with 30 compression cycles along the vertical direction.

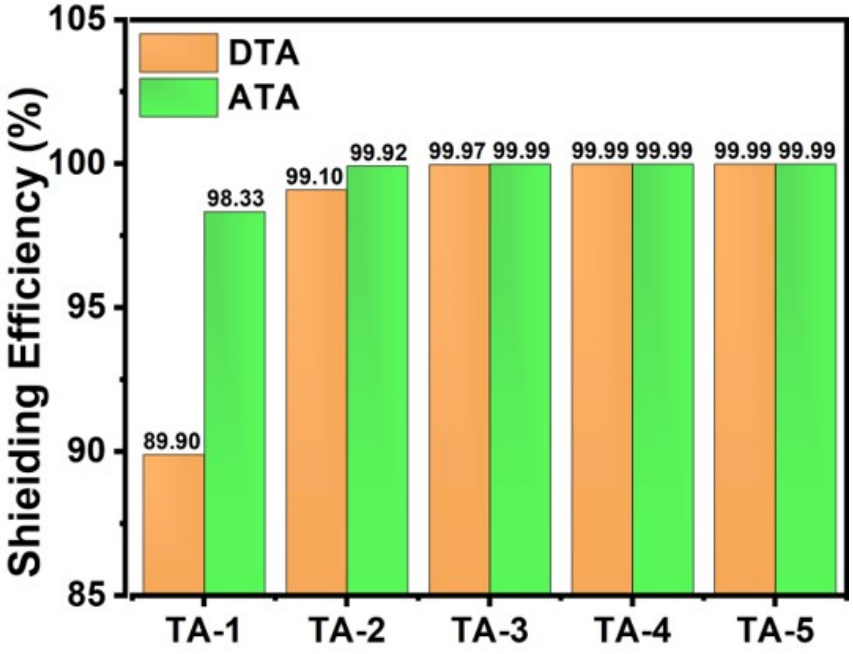

Figure S9. Comparison of electromagnetic shielding efficiency between disorder and anisotropy under different $Ti_3C_2T_x$ content.

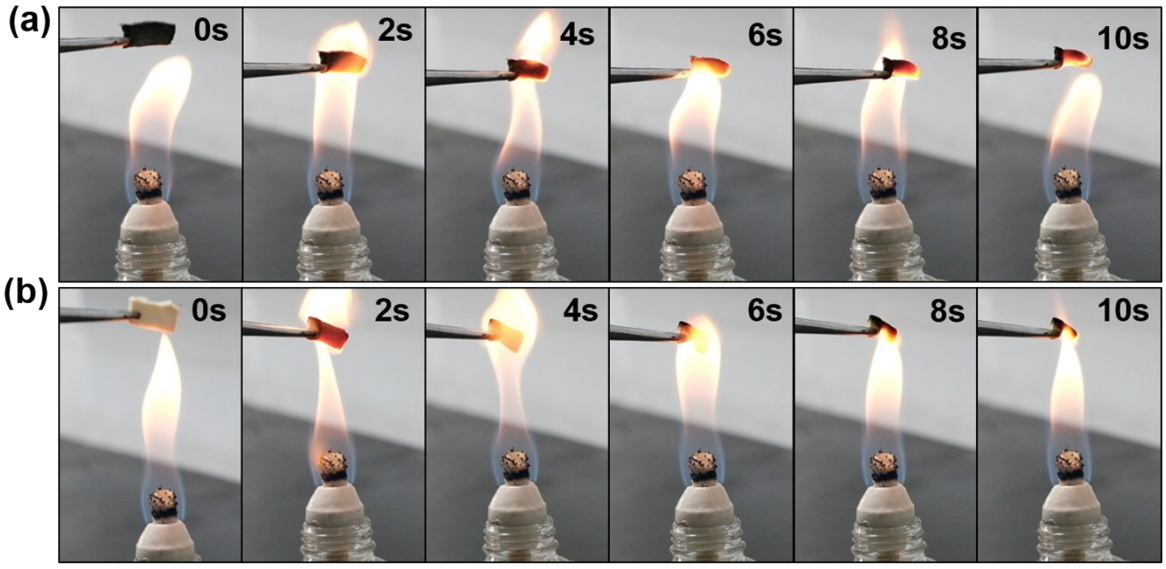

Figure S12. (a), (b) Photographs of aTA-3 and ANFs aerogel in the flame of an alcohol burner, respectively.

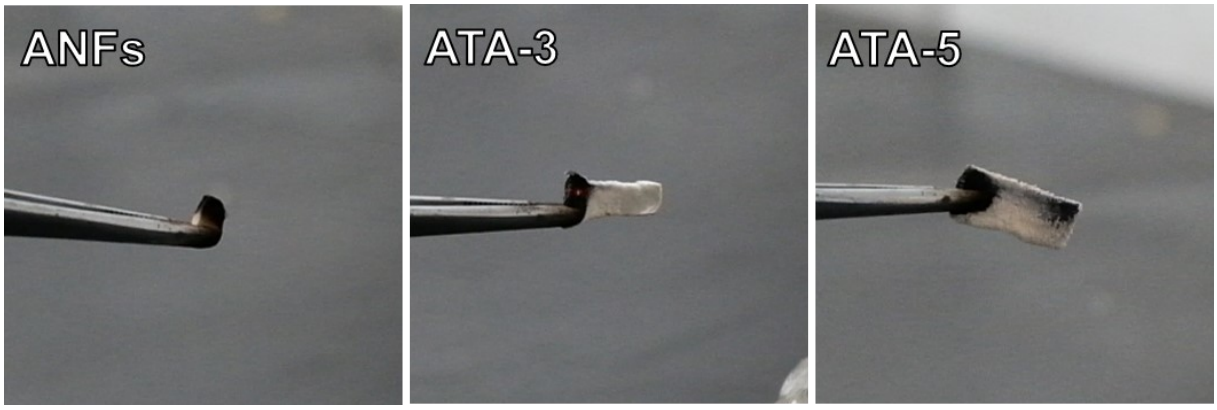

Figure S13. Digital photo of ANFs aerogel, aTA-3 and aTA-5 after burning, respectively.

Table S1. Comparison of EMI shielding performances of $Ti_3C_2T_x$/ANFs anisotropic aerogel with those of relevant composites reported in the literature.

Type		Sample	filler [Vol%]	t [mm]	ρ [g•cm^{-3}]	SE [dB]	SSE/t [dB·cm^{2}g^{-1}]	Ref.	ref
Aerogel structures	RGO	RGO/PEI	1.38	2.3	0.30	13	188	3	1
		RGO/PU	4.7	60	0.03	57.7	320	4	2
		RGO/PS	3.47	2.5	1.08	45.1	167.5	5	3
		RGO/PDMS	0.36	1	0.06	20	3333	6	4
	CNTs	MWCNT/WPU	7.2	4.5	0.13	50	881.8	7	5
		MWCNT/PLLA	1.47	2.5	0.30	23	306.7	8	6
		CNT/PS	3.6	0.12	5.61	18.5	275	9	7
		CNWs@G	4.6	1.6	0.10	36	2317	10	8
	Metal	CuNi	2.6	0.15	2.42	25	690	11	9
		CuNi-CNTs	2.6	0.15	2.30	54.6	1580	11	9
		Ag nanowires/PI	/	0.5	0.29	35	2416	12	10
		Ag@HGMs/Fe_3O_4	0.51	2		59		53	11
	MXene	$Ti_3C_2T_x$-RGO/Epoxy	0.99	2	0.30	56.4	940	24	12
		Ti_2CT_x/PVA	0.15	5	0.01	28	5136		13
		$Ti_3C_2T_x$/PS	1.9	2	1.21	62	255.2	1	14

		$Ti_3C_2T_x$	16.3	0.006	0.39	32	136752	2	[15]
		$Ti_3C_2T_x$	16.7	0.018	0.40	50	69444	2	[15]
		$Ti_3C_2T_x$/aCNT	0.59	2	0.02	90	24725		[16]
		$Ti_3C_2T_x$ aerogel/epoxy	0.4	2		34.5		55	[17]
		$Ti_3C_2T_x$ /AgNW		2	0.049	52.6	5313	72	[18]
		$Ti_3C_2T_x$ /CNT		3	0.042	104	8253	78	[19]
		aTA-5	0.58	2.5	0.02	65.5	11391		**This work**
		aTA-4	0.44	2.6	0.02	56.9	9515		**This work**
		aTA-3	0.29	2.5	0.02	44.7	7774		**This work**
Film structure	RGO	RGO/WPU	5	1	1.01	34	338	16	[20]
		RGO-Fe_3O_4/PVC	3.4	1.8	1.46	13	49.5	17	[21]
		RGO-γ-Fe_2O_3/PVA	2.3	0.36	1.35	20.3	416.7	18	[22]
		RGO/PANI	18.8			34.2	118.75	19	[23]
	CNTs	MWCNTs/Epoxy	1.34	2	1.99	40	100.5	20	[24]
		CNTs/PC	5	1.85	1.20	25	112.6	21	[25]
		CNTs/PP	7.5	1	0.94	35	372	22	[26]
		SWCNTs/PANI	15.5	2.4	1.30	31.5	100.8	19	[23]
		CNTs/PDMS	1.74	2		43		62	[27]
	Metal	Al Foil	100	0.008	2.70	66	30555	13	[28]
		Cu Foil	100	0.01	8.96	70	7812	13	[28]
	MXene	$Ti_3C_2T_x$	100	0.011	2.39	68	25863	13	[28]

		$Ti_3C_2T_x$ /SA	87	0.008	2.31	57	30830	13	**28**
		$Ti_3C_2T_x$ /CNFs	39.9	0.167	1.13	25	1326	14	**29**
		$Ti_3C_2T_x$ /CNFs	72.7	0.074	1.63	26	2154	14	**29**
		Ti_3C_2Tx/Wax	77.2	1	2.05	76.1	371	15	**30**
		MXene@NR	6.71	0.246		54		58	**31**
		$Ti_3C_2T_x$/PVA		0.027	1.74	44.4	9343	65	**32**

Calculation of volume fraction of $Ti_3C_2T_x$

The volume fraction of A is calculated based on the density of the components mentioned in the reported literature. [16] The true densities of $Ti_3C_2T_x$ is 3.2 mg/cm^3.

$$(\text{Vol }\%)_{\text{MXene}} = \boldsymbol{V}_{\text{MXene}} / \boldsymbol{V}_{\text{aTA}} \times 100\%$$

$$\boldsymbol{V}_{\text{MXene}} = \boldsymbol{m}_{\text{MXene}} / \boldsymbol{\rho}_{\text{MXene}}$$

Notes and references

1. J. Ling, W. Zhai, W. Feng, B. Shen, J. Zhang and W. Zheng, *ACS Appl. Mater. Interfaces*, 2013, **5**, 2677-2684.
2. B. Shen, Y. Li, W. Zhai and W. Zheng, *ACS Appl. Mater. Interfaces*, 2016, **8**, 8050-8057.
3. D.-X. Yan, H. Pang, B. Li, R. Vajtai, L. Xu, P.-G. Ren, J.-H. Wang and Z.-M. Li, *Adv. Funct. Mater.*, 2015, **25**, 559-566.
4. Z. Chen, C. Xu, C. Ma, W. Ren and H. M. Cheng, *Adv. Mater.*, 2013, **25**, 1296-1300.
5. Z. Zeng, H. Jin, M. Chen, W. Li, L. Zhou and Z. Zhang, *Adv. Funct. Mater.*, 2016, **26**, 303-310.
6. T. Kuang, L. Chang, F. Chen, Y. Sheng, D. Fu and X. Peng, *Carbon*, 2016, **105**, 305-313.
7. Y. Yang, M. C. Gupta, K. L. Dudley and R. W. Lawrence, *Nano Lett*, 2005, **5**, 2131-2134.
8. L. Kong, X. Yin, M. Han, X. Yuan, Z. Hou, F. Ye, L. Zhang, L. Cheng, Z. Xu and J. Huang, *Carbon*, 2017, **111**, 94-102.
9. K. Ji, H. Zhao, J. Zhang, J. Chen and Z. Dai, *Appl. Surf. Sci.*, 2014, **311**, 351-356.
10. J. Ma, K. Wang and M. Zhan, *RSC Adv.*, 2015, **5**, 65283-65296.
11. J. Yang, X. Liao, G. Wang, J. Chen, F. Guo, W. Tang, W. Wang, Z. Yan and G. Li, *Chem. Eng. J.*, 2020, **390**.
12. S. Zhao, H. B. Zhang, J. Q. Luo, Q. W. Wang, B. Xu, S. Hong and Z. Z. Yu, *ACS Nano*, 2018, **12**, 11193-11202.
13. H. Xu, X. Yin, X. Li, M. Li, S. Liang, L. Zhang and L. Cheng, *ACS Appl. Mater. Interfaces*, 2019, **11**, 10198-10207.
14. R. Sun, H.-B. Zhang, J. Liu, X. Xie, R. Yang, Y. Li, S. Hong and Z.-Z. Yu, *Adv. Funct. Mater.*, 2017, **27**.
15. J. Liu, H. B. Zhang, R. Sun, Y. Liu, Z. Liu, A. Zhou and Z. Z. Yu, *Adv. Mater.*, 2017, **29**.
16. Z. Deng, P. Tang, X. Wu, H. B. Zhang and Z. Z. Yu, *ACS Appl. Mater. Interfaces*, 2021, **13**, 20539-20547.
17. S. Shi, B. Qian, X. Wu, H. Sun, H. Wang, H. B. Zhang, Z. Z. Yu and T. P. Russell, *Angew. Chem.-Int. Edit.*, 2019, **58**, 18171-18176.
18. C. Weng, G. Wang, Z. Dai, Y. Pei, L. Liu and Z. Zhang, *Nanoscale*, 2019, **11**, 22804-22812.
19. P. Sambyal, A. Iqbal, J. Hong, H. Kim, M. K. Kim, S. M. Hong, M. Han, Y. Gogotsi and C. M. Koo, *ACS Appl. Mater. Interfaces*, 2019, **11**, 38046-38054.
20. S. T. Hsiao, C. C. Ma, W. H. Liao, Y. S. Wang, S. M. Li, Y. C. Huang, R. B. Yang and W. F. Liang, *ACS Appl. Mater. Interfaces*, 2014, **6**, 10667-10678.
21. K. Yao, J. Gong, N. Tian, Y. Lin, X. Wen, Z. Jiang, H. Na and T. Tang, *RSC Adv.*, 2015, **5**, 31910-31919.
22. B. Yuan, C. Bao, X. Qian, L. Song, Q. Tai, K. M. Liew and Y. Hu, *Carbon*, 2014, **75**, 178-189.
23. B. Yuan, L. Yu, L. Sheng, K. An and X. Zhao, *Journal of Physics D: Applied Physics*, 2012, **45**, 235108.
24. Y. Chen, H.-B. Zhang, Y. Yang, M. Wang, A. Cao and Z.-Z. Yu, *Adv. Mater.*, 2016, **26**, 447-455.
25. M. Arjmand, M. Mahmoodi, G. A. Gelves, S. Park and U. Sundararaj, *Carbon*, 2011, **49**, 3430-3440.
26. M. H. Al-Saleh and U. Sundararaj, *Carbon*, 2009, **47**, 1738-1746.
27. J.-H. Cai, J. Li, X.-D. Chen and M. Wang, *Chem. Eng. J.*, 2020, **393**.
28. F. Shahzad, M. Alhabeb, C. B. Hatter, B. Anasori, S. Man Hong, C. M. Koo and Y. Gogotsi, *Science*, 2016, **353**, 1137-1140.
29. W. T. Cao, F. F. Chen, Y. J. Zhu, Y. G. Zhang, Y. Y. Jiang, M. G. Ma and F. Chen, *ACS Nano*, 2018, **12**, 4583-4593.

30. M. Han, X. Yin, H. Wu, Z. Hou, C. Song, X. Li, L. Zhang and L. Cheng, *ACS Appl. Mater. Interfaces*, 2016, **8**, 21011-21019.
31. J.-Q. Luo, S. Zhao, H.-B. Zhang, Z. Deng, L. Li and Z.-Z. Yu, *Compos. Sci. Technol.*, 2019, **182**.
32. X. Jin, J. Wang, L. Dai, X. Liu, L. Li, Y. Yang, Y. Cao, W. Wang, H. Wu and S. Guo, *Chem. Eng. J.*, 2020, **380**.